International Journal of Mechanical Engineering and Applications
2022; 10(1): 7-16
http://www.sciencepublishinggroup.com/j/ijmea
doi: 10.11648/j.ijmea.20221001.12
ISSN: 2330-023X (Print); ISSN: 2330-0248 (Online)

Development of New Sound Insulation Simulation Technology Using Finite Element Method for Efficiency of High Aspect Ratio Core in Low Frequency Range

Abe Aya*, Ichiro Hagiwara

Meiji Institute for Advanced Study of Mathematical Sciences, Meiji University, Tokyo, Japan

Email address:

aya_abe@ meiji.ac.jp (A. Aya), ihagi@meiji.ac.jp (I. Hagiwara)

*Corresponding author

To cite this article:

Abe Aya, Ichiro Hagiwara. Development of New Sound Insulation Simulation Technology Using Finite Element Method for Efficiency of High Aspect Ratio Core in Low Frequency Range. *International Journal of Mechanical Engineering and Applications.* Vol. 10, No. 1, 2022, pp. 7-16. doi: 10.11648/j.ijmea.20221001.12

Received: February 18, 2022; **Accepted**: March 11, 2022; **Published**: March 18, 2022

Abstract: Nowadays, meta-materials are being studied to reduce vehicle interior noise. But it has not yet been found effective meta-materials at low frequencies below 500Hz. A panel with one core which has an excellent sound insulation where the higher the height of the core, the better the sound insulation characteristics have been founded. And so, depending on the core height, a structure with one core which is effective even at 500hz or less may be obtained. If the core height is high, it cannot be obtained by press forming, so the origami forming has been developed. Use of FEM which is versatile for shape of structure is effective for analysis of the plate with core or with sound absorbing material. Although the FEM analysis for sound insulation analysis was difficult, so far, two methods have been developed. Here these two methods to a flat plate and a flat plate with sound absorbing material to grasp their characteristics are compared and applied. And then the more versatile method is selected for sound insulation analysis to plates with one core which are formed by origami forming. As a result, it is shown that a plate with one core is effective for sound insulation characteristics at the low frequency below 500Hz depending on the balance between plate thickness and core height. At last, it is shown the core shape that maximizes the integral value of the sound insulation characteristic from 0 Hz to 500 Hz by an optimal analysis.

Keywords: Origami Forming, Origami Core, Optimal Analysis, Meta-material, Sound Absorbing Material, Helmholtz Equation

1. Introduction

The research with the aim of industrializing octet truss-type cores (truss cores) that use space filling structures composed of regular tetrahedrons and half regular octahedrons has been performed. [1-3]. Honeycomb cores have the disadvantages of high cost and a vulnerability to heat because of the gluing process required in their manufacture. In contrast, a truss core has the same bending stiffness as the honeycomb core and is manufactured by press forming only. In the case of a steel structure, the manufacturing cost is approximately one third of that of the honeycomb core and the resulting core remains strong against heat.

However, although the truss core was expected to replace the honeycomb core, it proved to be extremely difficult to form a good truss core with uniformly arranged cores in the case of a metal core structure. It was found that good molding results could be obtained using the Tokura-Hagiwara multi-stage press molding method [4]. Subsequently, truss cores have been used in solar panels and solar heliostats [5]. Furthermore, truss cores were expected to be used as flooring for trains, but both good sound insulation characteristics especially in low frequency range and bending stiffness are required for this application.

In addition, it has been reported that a higher core height produces better sound insulation characteristics in honeycomb cores [6]. However, there is a limit to the core height available in the multi-stage pressing approach mentioned above.

Therefore, the origami forming engineering method to solve the core height problem [7-9] are developed and then to

reexamine the sound insulation properties of these cores is decided.

There is a two-point microphone method [10] for estimation of sound insulation characteristics. With this method consideration is required for setting the position of microphone and even if the sound insulation characteristics become clear with this method, it needs to use FEM for improving characteristics. Although transmission matrix method [11] is also a method for estimation of sound insulation characteristics, this is limited to the test piece of which characteristics can be estimated theoretically.

Therefore, to use FEM for this problem is tried. Of course, there are many papers [12, 13] using FEM for estimation of sound insulation characteristics. As shown in these papers, there are no FEM papers for corresponding to the original definition of transmission loss. And so, this was examined using FEM by the second author et al. [14, 15], but a correction value was required to ensure that the results corresponded to the theoretical values. In addition, because the correction values differ depending on the type of test piece involved [14, 15], it is difficult to produce a quantitative measure of how much the sound insulation performance is improved in the case of a plate with cores when compared with a flat plate alone by using this type of simulation.

Therefore, in the previous paper [16], the reason why the results obtained by theory and FEM are different is clarified when the test piece can be regarded as a rigid body. Furthermore, it is firstly proved that the possibility of fusion of the finite difference method and the finite element method in this problem where the forward wave and the backward wave can be theoretically separated [17].

In this paper, these two methods to a flat plate and a flat plate with sound absorbing material to grasp their characteristics are compared and applied. And then the more versatile method is selected for sound insulation analysis to plates with one core which are formed by origami forming. As a result, it is shown that a plate with one core is effective for sound insulation characteristics at the low frequency below 500Hz depending on the balance between plate thickness and core height. At last, it is shown the core shape that maximizes the integral value of the sound insulation characteristic from 0Hz to 500Hz by an optimal analysis.

2. Calculation Method for Sound Insulation Characteristics Evaluation

In the model proposed by Ishida et al. [14, 15], the other end of the sound receiving side is set to be in the perfectly reflective condition. Determination of the cause of the difference between the theoretical and simulated values was described as a task for future work [14, 15]. The main cause of this difference was the failure to recognize that although the pressure is expressed using a combination of the forward waves and the backward waves when the Helmholtz equation representing the sound field is solved directly in the time domain, it is simply obtained as the sum of these waves in the FEM. In other words, the transmission loss is defined using the forward wave sound pressure on the receiving side with respect to the forward wave sound pressure on the sound source side. However, in the previous studies [14, 15], the sound pressure on the sound source side that was determined by the FEM was used as the forward wave sound pressure on the sound source side.

Therefore, in a specimen that is to be close to rigid, the pressures of the forward and backward waves are almost equal, and thus half of the sound pressure on the sound source side determined by the FEM is used as the input wave. Furthermore, by setting the other end of the sound receiving side to be a nonreflective boundary, the sound insulation is calculated using only the forward wave on the sound receiving side and results consistent with the theoretical value were then obtained [16].

However, this method cannot be applied when the specimen cannot be clearly regarded as being rigid, e.g., when assessing the effect of attaching a sound absorbing material to the specimen. Therefore, by using the value obtained via the FEM as a boundary condition, a calculation method that separates the forward wave and the backward wave accurately is developed from Helmholtz's theoretical solution.

Next, by comparing the results obtained with those from the previous paper [16], the validity of the method developed in this paper is confirmed in two cases; the first is when the specimen is regarded as a rigid body and the second is when the specimen is attached to a sound absorbing material, which is a difficult case to examine when using the previously reported method.

2.1. Examination of Sound Insulation Calculations

The definition of the transmission loss (TL) used in sound insulation calculations is the ratio of the energy of the incident sound wave to the energy of the transmitted sound wave. The equation (1) is used in this paper. p_{in} is the incident sound pressure, and p_{out} is the transmitted sound pressure as shown in Figure 1.

$$TL = 20 \log_{10} \frac{|p_{in}|}{|p_{out}|} \tag{1}$$

In the previous paper [16], the problem was solved when the specimen was a rigid body, and the magnitudes of the incident and reflected waves were equal. However, this method cannot be applied when the specimen cannot be clearly regarded as a rigid body, e.g., when the effect of attaching a sound absorbing material is to be analyzed. Therefore, a method to obtain the transmission loss by separating the incident sound pressure from the reflected sound pressure theoretically is studied here.

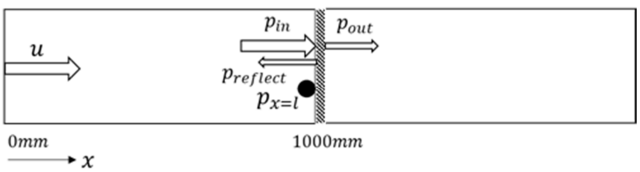

Figure 1. *Schematic model of the acoustic tube.*

2.2. Incident Sound Pressure Calculation Method in Sound Insulation Characteristic Simulation Method

Helmholtz's equation (2) holds in the acoustic tube model shown in Figure 1. [18]

$$\frac{\partial^2 u}{\partial x^2} = \frac{1}{c^2}\frac{\partial^2 u}{\partial t^2} \tag{2}$$

Here, u is the particle velocity, x is the one-dimensional position coordinate, and t is the time. The solution of Eq. (2) can be obtained by Eq. (3). Assuming a harmonic motion for the particle velocity,

$$u(x,t) = Ae^{j(\omega t - kx)} + Be^{j(\omega t + kx)} \tag{3}$$

Here, ω is the angular frequency, e is the Napier's constant, k is the wave number, and j is the imaginary unit. The first term on the right side represents the traveling wave component of the particle velocity, and the second term represents the backward wave component. Assuming that the amplitude of the particle velocity of the sound source plate is u_0, the particle velocity at $x=0$ can be expressed by Eq. (4).

$$u(0,t) = u_0 e^{j\omega t} \tag{4}$$

If the amplitude of the particle velocity of the sound insulation plate is D, the particle velocity at $x=l$ can be expressed by Eq. (5).

$$u(l,t) = De^{j\omega t} \tag{5}$$

From these conditions, the solution u becomes Eq. (6).

$$u(x,t) = \frac{u_0 e^{j2kl} - De^{jkl}}{e^{j2kl}-1} e^{j(\omega t - kx)} + \frac{De^{jkl} - u_0}{e^{j2kl}-1} e^{j(\omega t + kx)} \tag{6}$$

The incident sound pressure $p_{in}|_{x=l}$ is obtained by multiplying the particle velocity with x=l in Eq. (5) by the air density ρ and the sound velocity c, so it becomes Eq. (7).

$$p_{in}|_{x=l} = \rho c \cdot \frac{u_0 e^{jkl} - D}{e^{j2kl}-1} e^{j\omega t} \tag{7}$$

Here, D is obtained from Eqs. (4) and (5) to Eq. (8).

$$D = \frac{2u_0 e^{jkl}}{1+e^{j2kl}} + p_{x=l} \cdot \frac{1-e^{j2kl}}{\rho c\left(1+e^{j2kl}\right)} \tag{8}$$

Similarly, the reflected sound pressure $p_{reflect}|_{x=l}$ is given by Eq. (9).

$$p_{reflct}|_{x=l} = \rho c \frac{u_0 e^{jkl} - De^{j2kl}}{e^{j2kl}-1} e^{j\omega t} \tag{9}$$

3. Comparison of the Two Methods for Flat Plate Transmission Loss

Section 3.1 describes the model used in this study. Section 3.2 compares the two types of sound pressure: (1) the incident sound pressure when it is equal to the reflected sound pressure, and (2) the incident sound pressure obtained by the theoretical method in Section 2.2. A similar comparison of the transmission losses in these two cases is presented in Section 3.3.

3.1. Analysis Model

Figure 2 shows the simulation model used in this study. A flat plate is used as the test piece. COMSOL Multiphysics software [19] is used to perform the calculations. The lengths of the sound tube in front of and behind the sound insulation plate are both 1 m and the rear end on the sound receiving side is a nonreflective boundary. The boundary condition between the acoustic tube and the test piece is a free end. The air layer contained inside the acoustic tube uses solid elements, the test piece uses shell elements, the total number of elements is 640 (comprising 624 solid elements and 16 shell elements) and the number of nodes is 1025. The sound insulation plate is a steel plate with a thickness of 0.8 mm and the plate's material properties are listed in Table 1. The sound pressure observation point is located 1 mm in front of the sound insulation plate in the x-axis direction.

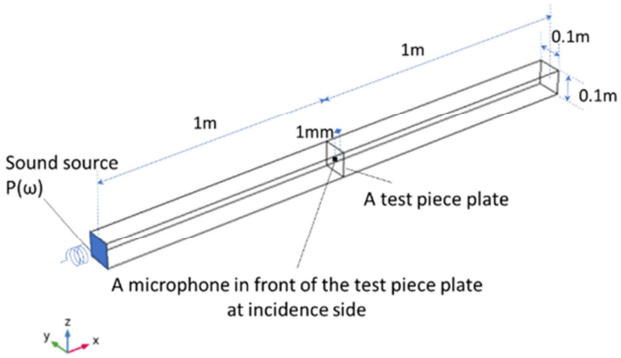

Figure 2. *Simulation model with the sound insulation plate.*

Table 1. *Specification of the plate material.*

Material	Young's modulus [N/m^2]	Density [kg/m^3]	Poisson ratio
Steel	2.05×10^{11}	7.85×10^{3}	0.28

3.2. Comparison of Sound Pressures

Figure 3 shows a comparison of the frequency response calculation values obtained for the incident sound pressure at the sound pressure observation points using the two methods. The figure compares the incident sound pressure (blue line) obtained as half of the FEM sound pressure value with the theoretically calculated value of the incident sound pressure (green line), which was obtained separately via the theoretical method. Because the sound insulation plate is a steel plate close to a rigid body, the incident sound pressure and the reflected sound pressure are almost identical over the entire frequency range, except in the range around 0 Hz. This pressure is almost half the value of the FEM sound pressure. As a result, it is verified that the incident wave and the reflected wave are equal and that the value of the incident wave used for the transmission loss is halved when the flat plate in Figure 3 can be regarded as a rigid body.

Additionally, the validity of the method developed in this paper is also verified. In Figure 3, the frequency for each

sound pressure shows peaks at regular intervals, which means that the half-wavelength multiples of the excited sound wave match the length of the acoustic tube. These peaks are present because resonant phenomena occur. Furthermore, in the theoretical calculation results for the incident sound pressure (green line), a peak that rises locally can be seen near the minimum value. These peaks are caused by the numerical calculations because the particle velocity diverges at a periodic frequency according to Eq. (6), which expresses the solution for the particle velocity u.

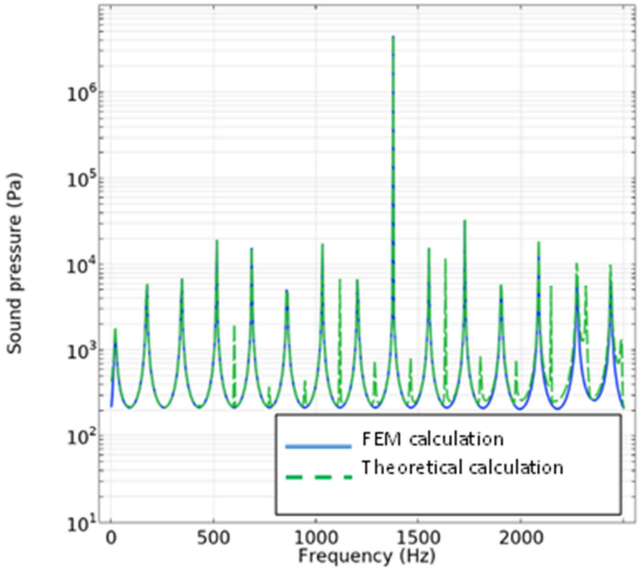

Figure 3. *Comparison of sound pressures of incident waves.*

3.3. Comparison of Transmission Losses

As with the case of the sound pressures, the transmission losses obtained by the two methods are compared. To calculate the transmission loss, the sound pressure values at points 1 mm in front of and behind the sound insulation wall are used on the sound source side and the sound receiving side, respectively. Figures 4 and 5 show comparisons of the transmission losses of flat plates determined using different mesh divisions. In Figure 4 of the coarse mesh division case (the total number of elements is 640 which consists of 624 solid elements and 16 shell elements as the same as Figure 2), the values tend to fluctuate slightly within the high frequency range; this seems to be an error due to the mesh division. In this case, the transmission losses of both methods fluctuate slightly up and down from approximately 1500 Hz or higher.

In contrast, in the fine mesh division case (the total number of elements is 1525 which consists of 1500 solid elements and 25 shell elements) shown in Figure 5, the transmission loss values for both methods are almost the same, even at frequencies of 2000 Hz or higher. As shown in both Figures 4 and 5, regard to the transmission losses obtained based on the theoretical value (green solid line), the local value increases occur at the frequency close to the point at which the denominator periodically becomes near-zero. This behavior can be explained using Eq. (6), which represents the solution for the particle velocity u. Except for these points, in the finer mesh division shown in Figure 5, both transmission loss values are almost identical at each frequency.

In other words, when the mesh is divided with a specified degree of fineness, the theoretically calculated characteristic value for the sound insulation of the flat plate is obtained as half the FEM sound pressure value except for some periodic local increases. It is then almost the same as the transmission loss that was obtained from the incident sound pressure value. Therefore, in the flat plate model, the validity of the assumption that the incident wave and the reflected wave are equal that was made in the previous paper [16] and the validity of the method proposed in this paper are both verified.

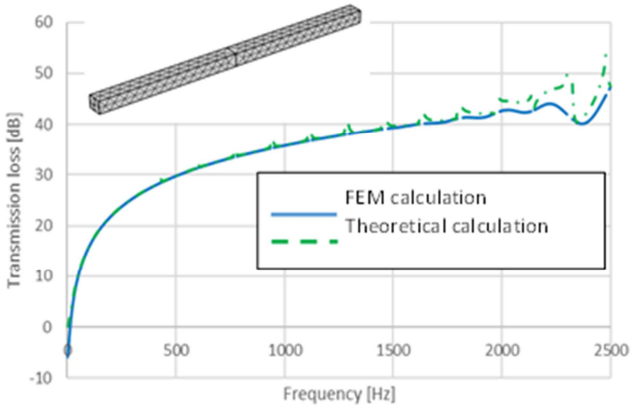

Figure 4. *Comparison of transmission loss with coarse elements.*

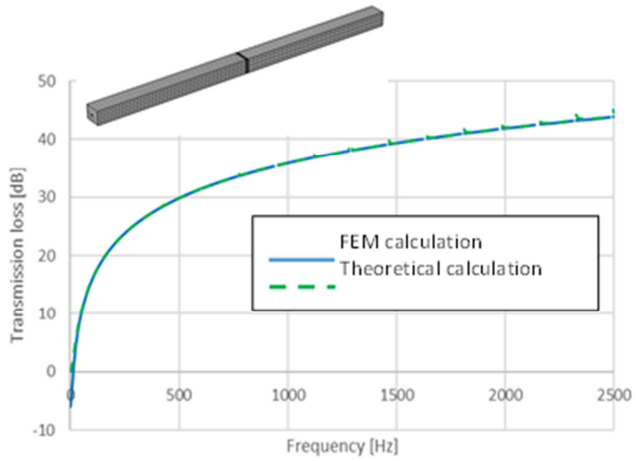

Figure 5. *Comparison of transmission loss with fine elements.*

4. Transmission Loss of Plate with Sound Absorbing Material

The case in which the sound absorbing material is attached to the entire flat plate surface on the sound source side will be examined from now. Glass wool with a fine fibrous structure is used as the sound absorbing material here. This wool is a fiber material that is sensitive to the particle velocity. As a result of the difference between the relative velocities of the fibers, friction heat is generated, and the acoustic energy is attenuated. The vertical incident sound absorption coefficient of the glass wool used here has the frequency response

characteristics shown in Figure 6 (plate thickness t of 25.0 mm, density ρ of 96.0 kg/m^3) and the model is based on this data. The analysis is performed by setting an approximate value for the acoustic impedance at each frequency.

4.1. Sound Pressure Calculation Results at Each Observation Point

The points used for the sound pressure calculations are the eight points shown in Figure 7. These points comprise four points on the sound source side and four points on the sound receiving side located at 0 mm, 300 mm, 600 mm, and 1000 mm (at the sound source side in the acoustic tube), and 1000.8 mm, 1300 mm, 1600 mm, and 2000 mm (at the sound receiving side in the acoustic tube), as measured from the left end of the sound source side. Figure 8 shows the results for the calculation values of sound pressure at p4 and p5, and that of particle velocity near vibration plate v1 and near the sound insulation plate v2, determined by the FEM and those results show the damping effect of the sound absorbing material. Furthermore, as shown in Figure 6, the sound absorption coefficient at the higher frequencies is high, thus indicating that the sound absorption effect of the glass wool is greater at higher frequencies.

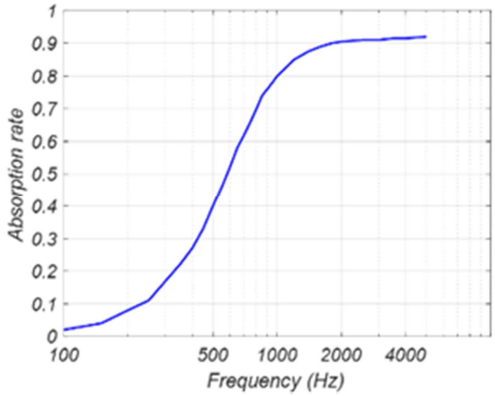

Figure 6. *Characteristics of the glass wool as sound absorbing material. Absorption rate vs. frequency.*

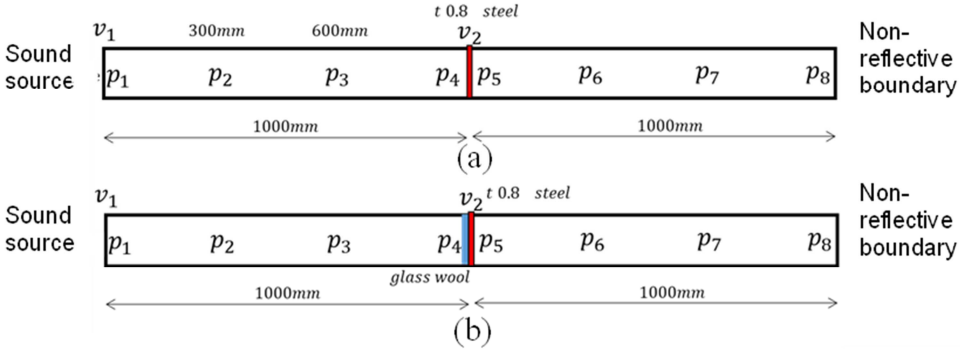

Figure 7. *Sound pressure observation points (a) without glass wool and (b) with glass wool.*

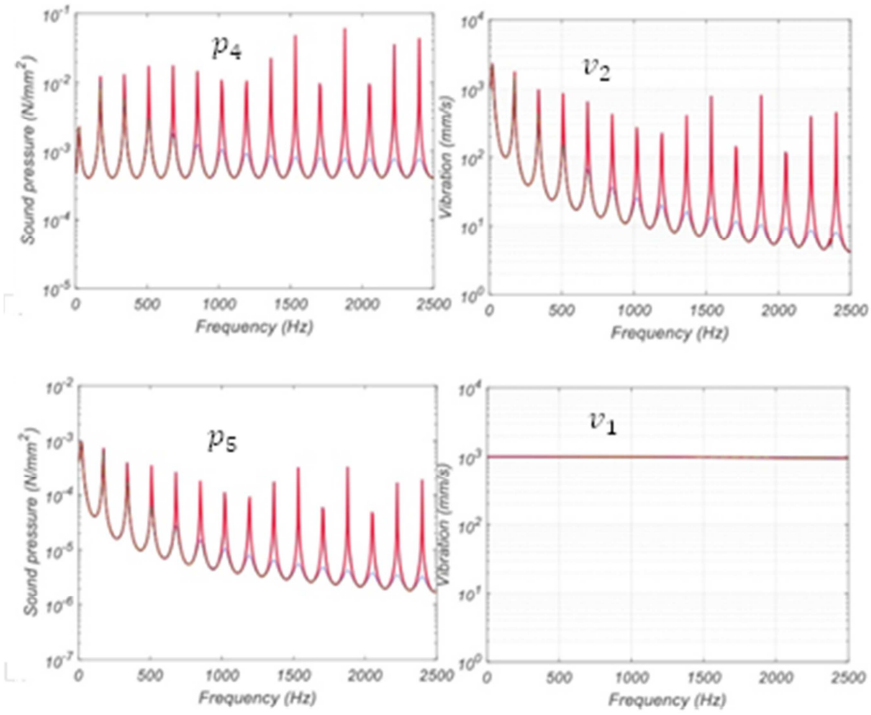

Figure 8. *Frequency responses of the sound pressures p_4 and p_5, and those of the particle velocities v_1 and v_2.*

4.2. Examination of Transmission Loss of Flat Plate with Sound Absorbing Material

When the flat plate with the sound absorbing material, as illustrated in Figure 9(a), is used as the sound insulation plate, the transmission losses are calculated using two methods and the results are compared. In Figure 9(b), based on the sound pressure values at points p4 and p5, the transmission losses are shown as calculated using the incident sound pressures (1) separated by the theoretical calculations (blue line) and (2) obtained as half of the FEM sound pressures (red line). The transmission losses determined by the two methods are both consistent with the behavior of a rigid body in the low frequency range, where the sound absorption effect is small. However, as the frequency increases, the sound absorption effect becomes larger. The transmission loss then becomes larger in (1) when compared with that in (2) by approximately 5 dB at around 2000 Hz, thus indicating that the effect of the sound absorbing material is reflected correctly by the calculation method in (1).

To confirm whether the method proposed in this paper is correct, the sound absorption characteristics are obtained from the transmission loss shown in Figure 9(b). Here, the definition of the vertical incident sound absorption coefficient α is used. α is obtained from Eq. (10). $E_{reflect}$ and E_{in} are the intensity of the reflected and the incident sounds respectively.

As shown in Figure 9(c), the vertical incident sound absorption coefficient (red line) calculated via the theoretical approach almost matches the sound absorption coefficient (blue line) of the glass wool and thus the coefficient is reproduced accurately using the method proposed here. Because the method used in the previous paper, in which it was simply assumed that the incident wave and the reflected wave were equal, meant that the case involving attachment of a sound absorbing material could not be examined, the result above indicates that the method developed in this paper is significant.

$$\alpha = 1 - E_{reflect} / E_{in} = 1 - |p_{reflect}|^2 / |p_{in}|^2 \quad (10)$$

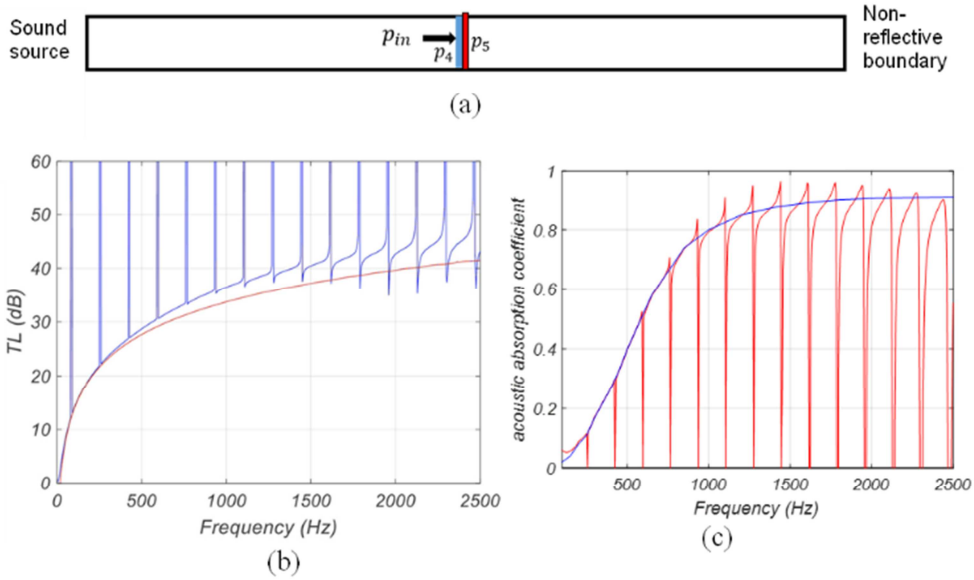

Figure 9. *(a) Model with sound absorbing Material; (b) Comparison of Transmission losses between theoretical (blue) and FEM calculations (red); (c) Comparison between theoretically calculated acoustic absorption coefficient (red) and the absorption rate (blue) of glass wool.*

5. Application to a Flat Plate with One Vertical Core

In Figure 9, it is shown that the sound absorption effect for sound insulation characteristics can be quantitatively obtained using glass wool as a sound absorbing material. Then, it is also shown that glass wool has a sound absorption effect at high frequencies, however it has little effect at low frequencies such as 500Hz or less. Therefore, to study the structure in which sound insulation characteristics can be obtained at low frequencies, the method developed in this paper is applied to the examination of the sound insulation characteristics of a flat plate with a single vertical core (hereinafter called a flat plate with a vertical core). First, the flat plate with a vertical core obtained by the origami forming method is described, and second, the comparison of sound insulation characteristics between a flat plate with a vertical core (4 cases of different aspect ratios) and a flat plate with equal mass conditions. It is examined lastly the core shape which gives the optimum value of sound insulation characteristics in the frequency range (0 - 500 Hz).

5.1. Flat Plate Model with One Vertical Core

An example of the shape of a flat plate with one vertical core is shown in Figure 10(a). In this paper, the aspect ratio h/a using the bottom length a of the core and the core height

h is defined. In the Tokura-Hagiwara paper [4], the plate thickness reduction rate in the press of the steel plate is explained by using the forming limit and formula. In the case of a = 65.5mm, the height h of Figure 10(a) is 16.4mm, the plate thickness reduction rate is 30%, and the aspect ratio up to 0.25 is the range that can be reached by the press. The core shape of Figure 10(b) has an aspect ratio of 0.56, which cannot be obtained by press forming, can be obtained by origami forming method [7-9]. As far as origami forming it was explained more in detail in Ref. [18].

In addition, considering that the flat plate with one vertical core as shown in Figure 10 is obtained in two dimensions with cross section by origami forming method, it is necessary to estimate the length twice the height h in the cross-sectional shape compared with the flat plate. Since thinking of comparing the plate with the same mass as the flat plate, the plate thickness should be adjusted by thinning.

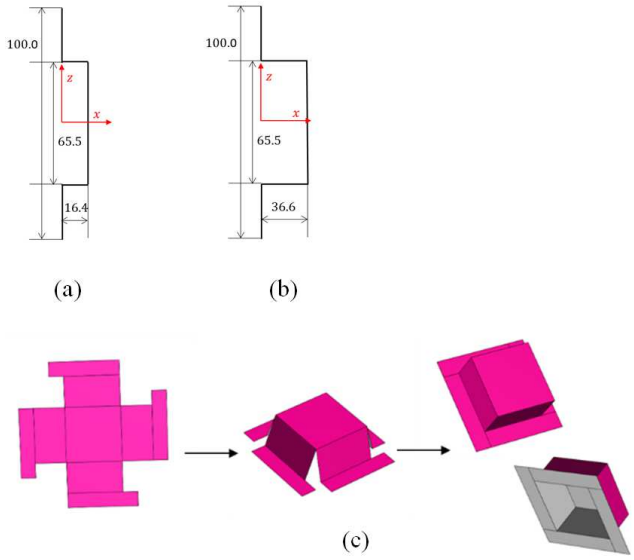

Figure 10. *Characteristics of the glass wool as sound absorbing material. (a) Enlarged image of glass wool, (b) Absorption rate vs. frequency.*

This paper shows a plan of the method of producing a flat plate with one vertical core. For vertical cores with a height that cannot be created by press forming from a flat plate, as shown in Figure 10(c), it is produced by using a low-cost and simple V-shaped tool that can perform folding line processing with a press that can be used for sharp bending and the origami forming method [9]. When the development diagram shown on the left is folded, a 3-dimensional shape shown on the right can be obtained through the shape in the middle.

5.2. Comparison of Sound Insulation Characteristics by Aspect Ratio Under Equal Mass Conditions of Flat Plates with a Vertical Core

Here, transmission loss of the flat plate with a vertical core as the same weight of a flat plate with a thickness of 0.8 mm is considered. To calculate the transmission loss, with the equation (7), the input wave and the reflected wave are separated by using the boundary conditions. At this time, the average sound pressure value of 1 cm in front of the plate is used as referred in the previous report [7]. As study cases, Case (a) is a possible shape by press forming as shown in Figures 11(a), and Cases (b) to (d) are produced by the origami forming method as shown in Figures 11(b), (c), (d). As a total, 4 cases are examined and are listed in Table 2.

Table 2. *Specification of 4 cases.*

Case	Core bottom length	Core height	Aspect ratio	Plate thickness
(a)	65.5mm	12.2mm	0.19	0.606mm
(b)	65.5mm	18.3mm	0.28	0.541mm
(c)	65.5mm	36.6mm	0.56	0.408mm
(d)	65.5mm	54.9mm	0.84	0.328mm

The comparison of transmission loss in 4 cases is shown in Figure 12. The case (d) which aspect ratio is the largest has a remarkable effect below 500 Hz. The slight effect is also obtained in cases (b) and (c), but no peaks below 500 Hz.

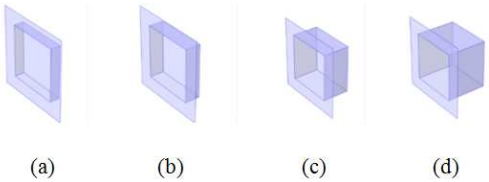

Figure 11. *4 shapes of the plate with a vertical core.*

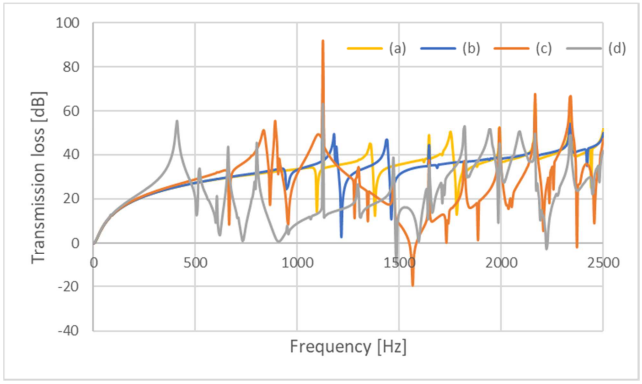

Figure 12. *Transmission loss in 4 cases.*

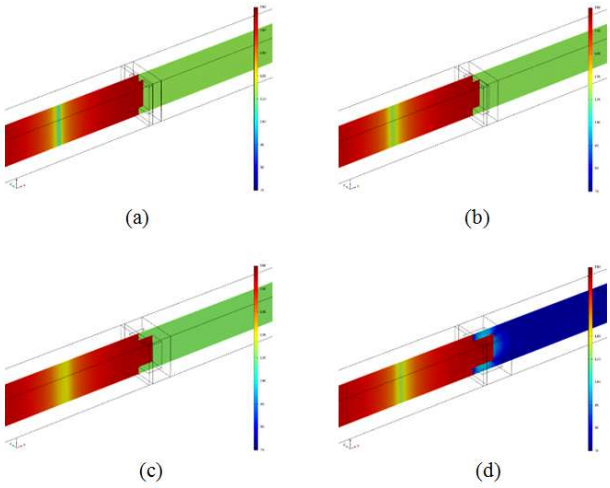

Figure 13. *Distribution of sound pressure level (dB) in 4 cases at 410 Hz.*

Figure 13 shows the distribution of the sound pressure level along the acoustic tube long hand cross section in 4 cases (a)-(d) at the frequency of 410 Hz. There is a large difference in the sound pressure level in front of and behind the sound insulation wall in case (d). In all cases, since the sound pressure level is observed to increase as the core height increases in front of the sound insulation wall (the red colors become darker), it is considered that a large collecting sound effect can be obtained by appropriately selecting the core height.

5.3. Examination of Core Height to Optimize Transmission Loss of Flat Plate with Vertical Core Under Equal Mass Conditions

As results in section 5.2, it is a good idea to improve sound insulation performance in the flat plate with one vertical core by appropriate aspect ratio in the low frequency range of 500 Hz or less where the sound absorption effect can hardly be obtained by glass wool. To reduce costs, the weight of the sound insulation material is tended to be suppressed. And so, if the height of the core is increased, the plate thickness will be set thin. Here the height (relating to aspect ratio) and thickness of this plate will be optimized under the equal mass condition at the lower frequency range than 500 Hz.

In this optimization analysis, the vertical core height h (10mm≦h≦100mm) of the plate is defined as a design variable, and to maximize the transmission loss integral value in the frequency range from 0 to 500 Hz is set as the objective function. The value of transmission loss is calculated by 5 Hz increments of frequency and then the area in the range between 0 and 500 Hz in trapezoidal law is obtained. The flowchart of optimization is shown as Figure 14. As a restraint condition, the mass is set about 62.8 g to be equal to the flat plate with a thickness of 0.8 mm, and the optimization solver uses a coordinate search method [20]. The convergence condition is shown as the equation (11).

$$\frac{\left|S^{n+1}_{TL(h)}[0,500]-S^{n}_{TL(h)}[0,500]\right|}{\left|S^{n}_{TL(h)}[0,500]\right|} \leq 0.0001 \qquad (11)$$

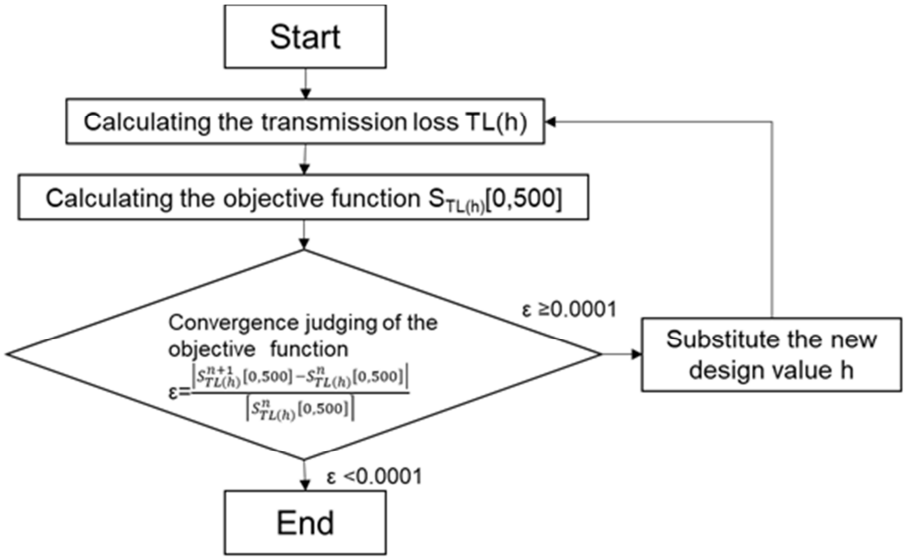

Figure 14. *Flow chart of the optimization analysis.*

As a result, as shown in Figure 15, the objective function is maximized when the number of iterations is 23. At that time, the optimized core height is 52.5 mm (thickness is 0.25 mm). Figure 16 compares the sound insulation characteristics of the flat plate with the optimized height core, and the flat plate with the equal weight in the frequency range of 0-500Hz.

There is an advantageous difference in sound insulation characteristics in the frequency range of about 150 Hz or more, and the maximum sound insulation effect can be obtained locally around 450 Hz.

Figure 17 shows the sound pressure level distribution of the acoustic tube long hand cross section around the sound insulation wall in the core shape obtained by optimization. At this time, it can be confirmed that there is a large difference (about 50 dB) in the sound pressure level in front of and behind the sound insulation wall.

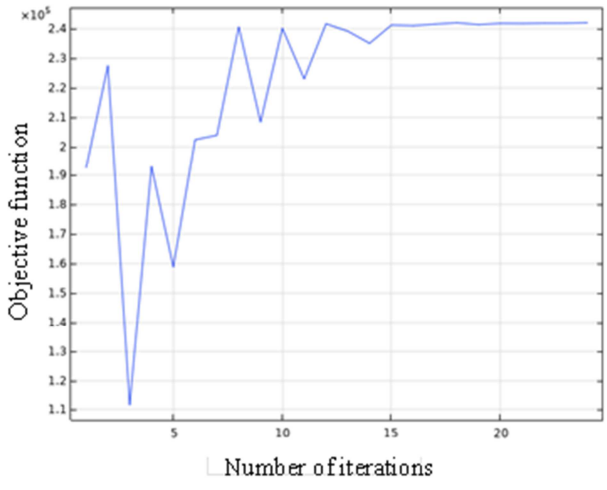

Figure 15. *Relationship between objective function and number of iterations.*

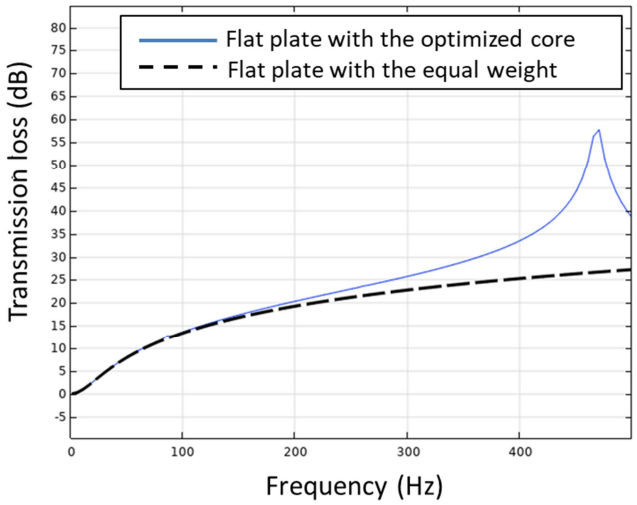

Figure 16. *Comparison of transmission loss.*

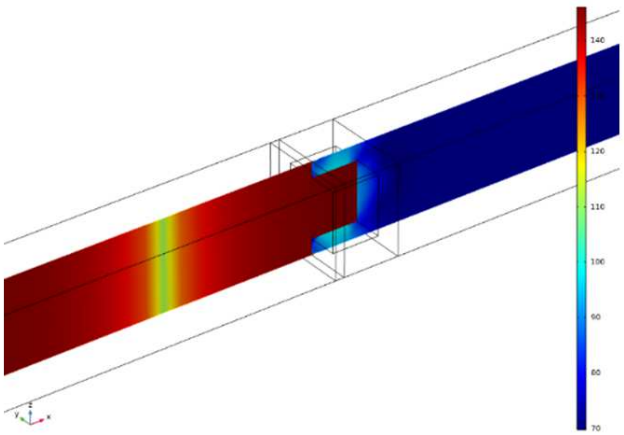

Figure 17. *Sound pressure distribution of the flat plate with an optimized core height.*

6. Conclusion

In the previous paper [16], the problem [14, 15] in which the difference of 6db was generated in FEM compared to the mass law of sound insulation was clarified by assuming that the incident wave and the reflected wave are equal in the flat plate model because it was difficult to separate the forward and the backward waves with the FEM. To generalize the separation method of the Helmholtz solution obtained by FEM into the incident wave and the reflected wave, we tried to develop a new method giving the FEM solution as a boundary condition to the differential decomposition expressed by the sum of the forward and the backward waves because in an acoustic tube with an extremely long one-dimensional direction, which can be regarded as one-dimensional behavior in the tube direction [17].

Here these two methods to a flat plate and a flat plate with sound absorbing material are compared and applied to grasp their characteristics. As far as the flat plate, these two methods give us the same results. But for the flat plate with absorbing material, the method by theoretical separation of FEM solution into the forward and backward waves gives us the excellent solution. And then this versatile method is selected for sound insulation analysis to plates with one core which are formed by origami forming. As a result, it is shown that a plate with one core is effective for sound insulation characteristics at the low frequency below 500Hz that cannot be compensated with sound absorbing materials and today's metamaterials [21] depending on the balance between plate thickness and core height. At last, it is shown the core shape that maximizes the integral value of the sound insulation characteristic from 0Hz to 500Hz by an optimal analysis.

Acknowledgements

This work is supported by the MIMS Joint Research Project (FY2020) for Mathematical Sciences, Meiji Institute for Advanced Study of Mathematical Science. The authors thank Dr. Mi Dahai from Keisoku Engineering System Co., Ltd. (https://kesco.co.jp/) for technical assistance with the application of COMSOL Multiphysics, and David MacDonald, MSc, from Edanz Group (https://en-author-services.edanz.com/ac) for editing a draft of this manuscript.

References

[1] Hagiwara, I., From Origami to 'Origamics', The Japan Journal, Vol. 5, No. 3 (2008-7), pp. 22-25 (in Japanese).

[2] Hagiwara, I., Stamping and welding two steel plates cheaper than honeycomb-panels, Automotive Technology (2011-1), pp. 96-101 (in Japanese).

[3] Terada, K. and Hagiwara, I., Freely manufacturing methods such as origami forming, Journal of the Japan Society of Mechanical Engineers (2016), Vol. 119, No. 1175, pp. 564-565 (in Japanese), DOI: 10.1299/jsmemag.119.1175_564.

[4] Tokura, S. and Hagiwara, I., Forming Process Simulation of Truss Core Panel, Journal of Computational Science and Technology, Vol. 4 (2010), No. 1, pp. 25-35 (in Japanese).

[5] Gotoh, Y. and Saito, K., Design and Manufacture of the Core Panel by Origami Engineering, Transactions of the Japan Society of Mechanical Engineers, Vol. 119, No. 1175 (2016-10), pp. 576-577 (in Japanese).

[6] Ng, C. F. and Hui, C. K., 'Low frequency sound insulation using stiffness control with honeycomb panels', Applied Acoustics, Vol. 69 (2008), pp. 293–301.

[7] Nguyen, H. T. T., Thai, P. T., Yu, B. and Hagiwara, I., Development of a Manufacturing Method for Truss Core Panels Based on Origami-forming, J. Mechanisms Robotics, (Dec 09, 2015), DOI: 10.1115/1.4032208.

[8] Terada, K., Kadoi, K., Tokura, S., Sushida, T. and Hagiwara, I., The deformation mechanism on origami-based foldable structures, Int. J. Vehicle Performance, Vol. 3, No. 4, 2017, pp. 334-346.

[9] Terada, K. and Hagiwara, I., Proposition of folding line processing by press method in origami forming, Transactions of the JSME (2021), Vol. 87, No. 898 (in Japanese), DOI: 10.1299/transjsme.21-00070.

[10] P. F Joseph, A two-microphone method for the determination of the mode amplitude distribution in high-frequency ducted broadband sound fields, The Journal of the Acoustical Society of America 142, 2019 (2017), DOI: 10.1121/1.5004568.

[11] Dell, A., KrynkinK, A. and Horoshenkov, V., The use of the transfer matrix method to predict the effective fluid properties of acoustical systems, Applied Acoustics, Volume 182, November 2021, 108259.

[12] Sophie, P., Maluski, S. and Gibbs, B. M., Application of a finite-element model to low-frequency sound insulation in dwellings, The Journal of the Acoustical Society of America, Vol. 108, No. 1741 (2000), DOI: 10.1121/1.1310355.

[13] Tomiku, R., Otsuru, T. and Takahashi, Y., Finite Element Sound Field Analysis of Diffuseness in Reverberation Rooms, Journal of Asian Architecture and Building Engineering, Vol. 1, No. 2 (2002), pp. 33-39 (in Japanese).

[14] Ishida, S., Morimura, H., Gotoh Y. and Hagiwara, I., New Transmission Loss Calculation Method Using Finite Element Method, Transactions of the Japan Society of Mechanical Engineers (2014), Vol. 80, No. 813 (in Japanese), DOI: 10.1299/transjsme.2014dr0127.

[15] Ishida, S., Morimura, H. and Hagiwara, I., Sound-Insulating Performance of Origami-based Sandwich Truss core Panels, Origami 6 (2016 1), pp. 431-438.

[16] Abe, A., Yashiro, H. and Hagiwara, I., Development of vertical incident sound insulation simulation technology using finite element method and application to lightweight core, Journal of the Society of Mechanical Engineers (2020) Vol. 86, No. 891, DOI: 10.1299/transjsme.20-00126 (in Japanese).

[17] Abe, A., Yashiro, H. and Hagiwara, I., Theoretical study of sound insulation simulations (about attaching effect of sound absorbing material and consideration of sound insulation performance by height of origami core), Proceedings of the ASME 2021 International Design Engineering Technical Conferences & Computers and Information in Engineering Conference IDETC/CIE 2021-68851.

[18] Suzuki, Y., Akagi, M., Ito, A., Sato, H., Yuki, A. and Nakamura, K., The Acoustical Society of Japan ed., Introduction to acoustics (2011), pp. 170-191, Corona Publishing (in Japanese).

[19] COMSOL Multiphysics® v. 5.5. www.comsol.com. (2019), COMSOL AB, Stockholm, Sweden.

[20] Conn, A., Scheinberg, K. and Vicente, L., Introduction to Derivative-Free Optimization (2009), MPS-SIAM Series on Optimization, SIAM.

[21] Kotaka, R. and Yamamoto, T., Dimension optimization of double wall acoustic metamaterial using resonator with thin membrane bottom, Dynamics & Design Conference 2020 (0), 352, 2020. (in Japanese).